Evaluation of initial collision-attachment efficiency between carbon dioxide bubbles and algae particles for separation and harvesting

Mi-Sug Kim and Dong-Heui Kwak

ABSTRACT

Microalgae have been regarded as a pollutant causing algal blooms in lakes or reservoirs but have recently been considered as a useful source of biomass to produce biofuel or feed for livestock. For the algae particle separation process, carbon dioxide (CO_2), one of the main greenhouse gases, is dissolved into a body of water rather than being emitted into atmosphere. This study aims at determining the feasibility of CO_2 bubbles as an algae particle separation collector in a flotation process and providing useful information for effective algae harvesting by describing optimal operating conditions of dissolved carbon dioxide flotation or dissolved air flotation. The first step is to develop a flotation model for bi-functional activity, algae control and algae harvesting at the same time. A series of model simulations is run to investigate algae particle separation possibilities such as an initial collision-attachment efficiency that depends upon separation characteristics due to an algae life cycle, including: pH, size distribution, zeta potential, cell surface charge, density, electric double layer, alkalinity, and so on. Based on the separation characteristics, conditions required to form flocculation are predicted in order to obtain the optimal flotation efficiency.

Key words | algae harvesting, bubble, carbon dioxide, flotation, particle separation

Mi-Sug Kim
Korean Urban Regeneration Technology Institute,
892-5 Inhu-1ga Deokjin-gu,
Jeonju 561-231,
Republic of Korea

Dong-Heui Kwak (corresponding author)
Dept of Env. and Chem. Eng.,
Seonam University,
439 Chunhyang-ro,
Namwon 590-711,
Republic of Korea
E-mail: *kwak124@hanmail.net*

INTRODUCTION

Extra attention has been focused on microalgae cultivation to produce various types of biofuel, given the competing demands between biofuel and food, the increase in crude oil price and the world-wide panic of a food shortage since 2003 (Demazel 2008). Algae have been mostly used as biological fertilizers and cultivated to feed animals and marine life (Chisti 2008). One of major microalgae used in biotechnology, *Spirulina*, reached about 3,500 tons of global production in 1999 as biomass. Ferrell & Valerie (2010) have stated that species such as *Spirulina* are easier to harvest because of their larger sizes, forming organized colonies that are similar in structure to filamentous microalgae. However, research on harvesting and separating microalgae varies on points of interests and technical approaches considerably. Applicable microalgae harvesting processes include centrifugation, sedimentation, flotation, filtration, membrane separation, etc., and algae separation studies have been performed on algae control or water treatment by water treatment engineers primarily (Kwak *et al.* 2011) and on algae harvesting as a source of biofuel for industry recently. Flotation is a very useful set of techniques, including auto-flotation, dissolved air flotation (DAF), and so on (Wiley *et al.* 2009; Xu *et al.* 2010). Also, dissolved carbon dioxide flotation (DCF) using one of the major greenhouse gases, carbon dioxide (CO_2), instead of air has the merit of CO_2 fixation. In DCF, CO_2 is not emitted into the atmosphere but dissolved in water and the fixed CO_2 becomes a carbon resource for algae growth. If no coagulants are applied in a flotation technique such as DCF, DCF can harvest much purer microalgae.

Flotation as a new green technology should be evaluated for its feasibility in managing and harvesting large amounts of microalgae. To evaluate flotation feasibility, a flotation modelling study may be appropriate because it reduces the cost and time in measuring and estimating optimal conditions for designing and operating flotation in real

doi: 10.2166/wst.2014.171

fields. This study aims at determining the feasibility of CO_2 bubbles as an algae particle separation collector in a flotation process and providing useful information for effective algae harvesting as drawing by describing optimal operating conditions of DCF or DAF. For that purpose, this study develops and validates a single-collector model (SCM) for collision-attachment efficiency as the fundamental flotation model, which becomes the initial datum of the population balance in turbulence (PBT) model described in many studies (Edzwald 2010). As the first step to achieving the two functions of algae management and algae harvest at the same time, this study aims at effectively analyzing and estimating the initial collision-attachment coefficient due to a life cycle of *Spirulina*. In this study, SCM simulation for DCF without dosing coagulants, as the harvesting technique has been conducted to investigate physical and chemical characteristics such as pH, zeta potential, cell surface charge, particle size, alkalinity, etc., and to provide optimal conditions for DCF in the laboratory.

MODEL DESCRIPTION

Flotation induces solid–liquid separation through rising aggregates of solids suspended in the dispersion medium and micro bubbles attached to the limited solid's surface, an interface of the dispersion medium and air. In the flotation process, bubbles are distributed in the range of about 10–120 μm (Edzwald 2010) and these bubbles float by buoyancy. Physical behavior includes attachment of the bubble, trapping of the rising bubble, and absorption and adsorption of the bubble by the particle's structure (Packham & Richards 1972). In predicting a flotation rate based on first principles, it is essential to consider parameters of interaction between the particle and bubble, hydrodynamics and surface forces. Among three subprocesses of the interaction including collision, attachment, and desorption, hydrodynamics caused by collision have been widely studied by many investigators and the results are useful in designing the flotation cells and scaling them up. The attachment process is less well understood because it is essentially controlled by complicated and difficult system chemistry. However, it is possible to determine attachment probability due to induction time, which is measured experimentally under different chemical conditions. According to the literature on the hydrophobic forces of particles and bubbles, attachment probability can be predicted using various parameters of surface chemistry. Although particles collide with bubbles, not all of them float as a result. Only hydrophobic particles are attached on the bubble surface. Thus, the attachment probability determines the selection of the flotation process, while its efficiency depends upon the collision efficiency. Also, some of the particles in the flotation cells are conducted by desorption from the bubble surface in turbulence and by inertia. Two processes, attachment and desorption, in the flotation cells are highly determined by particle–bubble surface chemistry. However, it is difficult to predict the probability of the subprocesses using parameters of surface chemistry such as contact angle, zeta potential, Hamaker constant, and so on.

This study focuses on the approach of a particle bumping on the bubble surface in order to estimate the collision efficiency between the particle and bubble. For trajectory analysis by a flow stream function, the model programmed in this study (SCM) has several assumptions and conditions as follows: (1) algae and bubbles are spherical; (2) the bubble radius is much greater than the algal radius and then the bubble surface over a short distance is assumed to be locally flat; (3) algae are suspended in water, algal disturbance is limited in the very small range in which algae are in the hydrodynamics of the bubble, and there is no effect on the velocity term of the fluid around the bubble; and (4) only intercept collisions in the Stokes flow are considered. Based on these assumptions and conditions, model equations are described in Table 1 as a function of force and velocity interacting between the particle and bubble, expressed by non-dimensional variables.

For understanding the balance of forces between the bubble and algae it is reasonable to describe the relationship between surface forces and hydrodynamics in the fluid. Kwak & Kim (2013b) have considered small algae flowing around the surface of a much larger bubble floating upward in fluid, described as Case A of Table 1, with detailed expression of the model equations. This study adds Case B, which considers the smaller collector flowing around the larger algal surface suspended in fluid, marked as Case B in Table 1, because the algae aggregated by auto-flocculation can be larger than the bubble. Based on Case B, SCM can be expressed by a non-dimensional distance (H), a radius ratio (R) of the bubble and algae, fluid velocities in the tangential direction and normal direction (V_θ and V_r) acting on the bubble surface flowing around the algal surface, and the total force combining the inter-particle surface force and the hydrodynamic force. In Table 1, the electrostatic force (F_{el}) is derived by Hogg *et al.* (1966) as a function of inverse Debye length (κ), the zeta potentials of the bubble and the particle (ζ_b and ζ_p),

Table 1 | SCM equations for trajectory analysis

Parameters/ variables	Model equations	
	Case A (particle radius, $r_p \ll$ bubble radius, r_b)	**Case B (particle radius, $r_p \gg$ bubble radius, r_b)**
A radius ratio of a bubble and a particle	$R = \frac{r_p}{r_b}$	$R = \frac{r_b}{r_p}$
Non-dimensional distance	$H = \frac{h}{r_p}$ $\bar{r} = \frac{r}{r_b}$ $= \frac{r_p + r_b + h}{r_b}$ $= R + 1 + HR$	$H = \frac{h}{r_b}$ $\bar{r} = \frac{r}{r_p}$ $= \frac{r_p + r_b + h}{r_p}$ $= 1 + R + HR$
Normal fluid velocity ($m\ s^{-1}$)	$V_r = r_p \frac{dH}{dt} = \frac{F_n f_1}{6\pi\mu r_p}$ [Case A] $V_r = r_b \frac{dH}{dt} = \frac{F_n f_1}{6\pi\mu r_b}$ [Case B]	Equation (1)
Tangential fluid velocity ($m\ s^{-1}$)	$V_\theta = r\frac{d\theta}{dt} = \mu_\theta f_3$	
Total force ($J\ m^{-1}$)	$F_n = F_{el} + F_{vdw} + F_{HP} + F_H$	Equation (2)
Electrostatic force ($J\ m^{-1}$)	$F_{el} = \frac{\varepsilon\varepsilon_0 r_b r_p}{4(r_b + r_p)}\left[\frac{4\zeta_b\zeta_p\kappa\exp(-\kappa r_b H)}{1+\exp(-\kappa r_b H)} - \left(\zeta_b^2 + \zeta_p^2\right)\frac{2\kappa\exp(-2\kappa r_b H)}{1-\exp(-2\kappa r_b H)}\right]$	Equation (3)
Van der Waals force ($J\ m^{-1}$)	$F_{vdw} = -\frac{A r_p}{6(r_b + r_p)h}$	Equation (4)
Hydrophobic force ($J\ m^{-1}$)	$F_{HP} = -\frac{K_{132} r_p}{6(r_b + r_p)h}$	Equation (5)
Hydrodynamic force	$F_H = 6\pi\mu r_p u_r;\ F_H = -\frac{3R^2(H+1)^2}{2(1+HR+R)^2} \times 6\pi\mu r_p u_b \cos\theta f_2$ [Case A] $F_H = 6\pi\mu r_b u_r f_2;\ F_H = -\frac{3R^2(H+1)^2}{2(1+HR+R)^2} \times 6\pi\mu r_b u_b \cos\theta f_2$ [Case B]	Equation (6)
Stream function	$\psi = \frac{3}{4} u_b (r - r_b)^2 sin^2\theta$	Equation (7)
Normal velocity	$u_r = -\frac{1}{r^2 \sin\theta}\frac{\partial\psi}{\partial r} = -\frac{3R^2(H+1)^2 u_b cos\theta}{2(1+HR+R)^2}$	Equation (8)
Tangential velocity	$u_\theta = \frac{1}{r \sin\theta}\frac{\partial\psi}{\partial r} = \frac{3R(H+1)}{2(1+HR+R)} \times u_b \sin\theta$	Equation (9)

(*continued*)

Table 1 | continued

Parameters/ variables	Model equations	
	Case A (particle radius, $r_p \ll$ bubble radius, r_b)	**Case B (particle radius, $r_p \gg$ bubble radius, r_b)**
Non-dimensional distance change in time change	$\frac{dH}{dt} = \frac{f_1}{6\pi\mu r_p^2} \times \left\{ \left[-\frac{Ar_b}{6(r_b+r_p)h} \right] + \left[\frac{\varepsilon\varepsilon_0 r_b r_p}{4(r_b+r_p)} \left[\frac{4\zeta_b\zeta_p\kappa\exp(-\kappa h)}{1+\exp(-\kappa h)} - \left(\zeta_b^2+\zeta_p^2\right)\frac{2\kappa\exp(-2\kappa h)}{1-\exp(-2\kappa h)} \right] \right.$ $\left. + \left[-\frac{K_{132}r_b}{6(r_b+r_p)h} \right] \right] + \left[-\frac{3R^2(H+1)^2}{2(1+HR+R)^2} \times 6\pi\mu r_p u_b \cos\theta f_2 \right] \right\}$ [Case A]	Equation (10)
	$\frac{dH}{dt} = \frac{f_1}{6\pi\mu r_b^2} \times \left\{ \left[-\frac{Ar_p}{6(r_b+r_p)h} \right] - \left[\frac{\varepsilon\varepsilon_0 r_b r_p}{4(r_b+r_p)} \left[\frac{4\zeta_b\zeta_p\kappa\exp(-\kappa h)}{1+\exp(-\kappa h)} - \left(\zeta_b^2+\zeta_p^2\right)\frac{2\kappa\exp(-2\kappa h)}{1-\exp(-2\kappa h)} \right] \right.$ $\left. + \left[-\frac{K_{132}r_b}{6(r_b+r_p)h} \right] \right] + \left[-\frac{3R^2(H+1)^2}{2(1+HR+R)^2} \times 6\pi\mu r_b u_b \cos\theta f_2 \right] \right\}$ [Case B]	
Tangential velocity with time change	$\frac{d\theta}{dt} = \frac{3R(H+1)}{2r(1+HR+R)} \times u_b \sin\theta f_3$	Equation (11)
Final model formula for the trajectory analysis	$\frac{dH}{d\theta} = \frac{2(1+HR+R)^2}{3R^2(H+1)} \frac{f_1}{6\pi\mu r_p u_b \sin\theta f_3} \times \left\{ \left[-\frac{Ar_b}{6(r_b+r_p)h} \right] - \left[\frac{\varepsilon\varepsilon_0 r_b r_p}{4(r_b+r_p)} \left[\frac{4\zeta_b\zeta_p\kappa\exp(-\kappa h)}{1+\exp(-\kappa h)} - \left(\zeta_b^2+\zeta_p^2\right)\frac{2\kappa\exp(-2\kappa h)}{1-\exp(-2\kappa h)} \right] + \left[-\frac{K_{132}r_b}{6(r_b+r_p)h} \right] \right] \right.$ $\left. + \left[-\frac{3R^2(H+1)^2}{2(1+HR+R)^2} \times 6\pi\mu r_p u_b \cos\theta f_2 \right] \right\}$ [Case A]	Equation (12)
	$\frac{dH}{d\theta} = \frac{2(1+HR+R)^2}{3R^2(H+1)} \frac{f_1}{6\pi\mu r_b u_b \sin\theta f_3} \times \left\{ \left[-\frac{Ar_p}{6(r_b+r_p)h} \right] \cdot \right.$ $\left. - \left[\frac{\varepsilon\varepsilon_0 r_b r_p}{4(r_b+r_p)} \left[\frac{4\zeta_b\zeta_p\kappa\exp(-\kappa h)}{1+\exp(-\kappa h)} - \left(\zeta_b^2+\zeta_p^2\right)\frac{2\kappa\exp(-2\kappa h)}{1-\exp(-2\kappa h)} \right] + \left[-\frac{K_{132}r_b}{6(r_b+r_p)h} \right] \right] + \left[-\frac{3R^2(H+1)^2}{2(1+HR+R)^2} \times 6\pi\mu r_b u_b \cos\theta f_2 \right] \right\}$ [Case B]	
Collision-attachment efficiency	$\eta_T = E_c E_a = \left[\frac{3}{2}\left(\frac{r_p}{r_b}\right)^2 \right] \left[\frac{X_c^2}{(r_p+r_b)^2} \right]$ [Case A] $\eta_T = E_c E_a = \left[\frac{3}{2}\left(\frac{r_b}{r_p}\right)^2 \right] \left[\frac{X_c^2}{(r_p+r_b)^2} \right]$ [Case B]	Equation (13)

the bubble radius (r_b), the particle radius (r_p), the permittivity (ε), and the permittivity of vacuum (ε_0). The van der Waals force (F_{vdw}) uses the formula of Ho & Higuchi (1968) related to the Hamaker constant (A), and the hydrophobic force (F_{HP}) is similar the van der Waals force and depends on the hydrophobic constant (K_{132}) (Firouzi *et al.* 2011). Also, the hydrodynamic force F_H is represented as Equation (6), where u_r is equal to the fluid velocity V_r acted in the normal direction of the algae and bubble. The stream function ψ of the equation for the trajectory analysis applies the formula of Levich (1962), where u_b represents the bubble velocity in the fluid. If the bubble and algae do not adhere to each other after the bubble moves toward the algae from the initial horizontal direction distance X, the θ value is used to perform numerical analysis with the increment $\Delta\theta = 0.1^\circ$ and calculate a critical distance X_c, the X-direction distance from the initial θ for the collision-attachment of the bubble and algae. Equation (13) is a formula to calculate the collision-attachment efficiency from the critical distance X_c, and the sizes of the algae and bubbles.

Total flotation probability of the particle by the bubble is expressed as a function of collision (P_c), attachment (P_a), stable three-phase contact formation (P_{TPC}), and stability of adsorption (P_{Stab}) as follows: $P = P_c P_a P_{TPC} P_{Stab}$. The collision probability P_c and the attachment probability P_a are strongly dependent upon the fluid dynamics of the system, while the other two probabilities are dependent on surface phenomena and assumed to have unit value, that is $P_{TPC} \approx 1$ and $P_{Stab} \approx 1$. Therefore, the total flotation probability can be simply rewritten as $P = P_c P_a$. Probability P_c is calculated by the hydrodynamics of the system related to the sizes of the particle and bubble. Nguyen (2011) summarizes collision probability models of the bubble–particle. Also, P_a is affected more by the surface chemical function than by the hydrodynamics. Probability P_a without the inertial force considers the particle to have a low mass density and assumes that the particle follows streamlines flowing around the bubble. This study used the Gaudin (1957) equation for P_c, equal to E_c in Equation (13), for the collision probability (or efficiency) using the stream function. Of course, Gaudin's equation underestimates P_c but it is useful for bubbles less than approximately 100 μm in diameter and for Stokes flow. Probability P_a of the special algae can be expressed as E_a in Equation (13). This form of the collision-attachment efficiency, as calculated in this study, can be applied as the initial collision-attachment coefficient in the PBT to estimate the flotation efficiency of the algae.

RESULTS AND DISCUSSION

Many previous studies reported that the interaction between the particle and bubble during flotation was influenced by hydrodynamics in the mass media of the water system. This study aimed at investigating the effect of the hydrodynamic force and the surface forces interacting over the short distance between the particle and bubble. The SCM model solved the entire equation for particle motion interacting around a bubble with immobile surface in the Stokes flow. The final differential equation for the trajectory analysis ($dH/d\theta$) was discontinuously solved according to the sequence of the Runge-Kutta method using Matlab Software. SCM began with an initial algae or bubble position, calculated with an assumption that the algae velocity was constant when far from the bubble surface and then the algae sedimentation velocity was equal to the fluid velocity. Initial y-direction values represented the non-dimensional initial distance H as the vertical distance of the bubble and algae, and established an initial value 20, an almost infinite level, while the x-direction was set by the tangent θ and the vertical distance H. The angle θ was used to perform numerical analysis with the increment $\Delta\theta = 0.1^\circ$ and a critical x-direction distance X_c was calculated from the initial θ for the collision-attachment of the bubble and algae. The collision-attachment probability P, using the critical distance X_c in Equation (13), was applied as the initial collision-attachment efficiency, one of input factors for the PBT model, to predict and estimate the flotation efficiency of the algae continuously.

Analysis of measured bubble sizes indicated different distributions according to whether coagulants were added (Kwak & Kim 2013a). Difference in bubble sizes depended upon the addition of coagulant. Bubbles were generated when the pressure was decreased in switching the processes from the saturator to the flotation basin. Bubble size when adding coagulants decreased because the surface tension of the bubble was reduced by the coagulants. Fine bubbles about 30 μm in diameter were constantly formed by the coagulant until the pressure was 2 atm and then proportionally swung upward as the surface tension was reduced for pressures 2 atm. To examine the effects of particle density, particle size, and film thickness for collision efficiency between the bubble and microalgae, the standard simulation condition of this study is presented in Table 2.

According to the literature, the *Spirulina* cell size was in the range 9 ± 2.5 μm and its zeta potential led −45 mV

Table 2 | Simulation conditions to examine collision efficiency

Parameters	Value	Unit	Parameters	Value	Unit
Algae radius	3.5–42	μm	K_{132}, hydrophobic constant	6.30×10^{-19}	J
Bubble radius	42	μm	$C_{H,}$ Hamaker constant	-3.12×10^{-21}	J
Bubble zeta potential	−25	mV	Water density	1,000	kg m^{-3}
Algae zeta potential	−45–45	mV	Bubble density	1.174	kg m^{-3}
Ion strength	0.003	mole m^{-3}	Algae density	473.4	kg m^{-3}
Viscosity	0.001	kg m^{-1} s^{-1}			

shortly before auto-flocculation. The simulations in this study used a bubble characterized by density 1.17 kg m^{-3}, zeta potential −25 mV, and representative bubble radius 42 μm in the typical range 20–60 μm. The microalgae were distributed from the smallest size of 3.5 μm in radius to the same as the bubble size, which was flocculated after adding coagulants. The microalgal zeta potential was applied from −45 to 45 mV. The collision-attachment efficiency P was examined with the parameters in Table 2. Figure 1(a) shows the collision efficiency indicating exponential growth as the algal aggregate grew larger and the attachment efficiency increased linearly for Case A. The collision-attachment efficiency was dependent on both the collision efficiency and the attachment efficiency. The collision efficiency was exponentially controlled by the algal size and the bubble size, while the attachment efficiency was linearly dependent on the critical distance X_c. In Figure 1(a), the limited critical distance, X_c, is proportionally increased as the algae aggregate is increased under the conditions of Case A. Also, the collision-attachment efficiency was the product of the collision efficiency and the attachment efficiency with an exponential increment.

As shown in Figure 1(b), the collision-attachment efficiency was controlled by the algal size and its zeta potential. To run the sensitivity simulations of the algal zeta potential, the efficiencies were calculated as changing the algal zeta potential from −45 to 45 mV in ranges of the algal radius from 3.5 μm to the same size as the bubble. It increased with growth of algae into aggregates and of algae zeta potential into positive values, and the larger size of the algal aggregates led to the wider amplification of the collision-attachment efficiency due to the algal zeta potential. The efficiency tended to increase as the zeta potential was close to the positive value and it decreased as the magnitude of negative value grew. Since the bubble zeta potential was in the negative range at −25 mV, the lowest collision-attachment efficiency was found when both values were in the negative range and was highest when the algal zeta potential was positive and the bubble zeta potential was negative. The difference between the highest and the lowest increased as the algal size grew gradually.

To examine the algal size effect due to different bubble sizes and to simulate the bubble size effect due to different algal sizes, all conditions of input parameters followed the standard simulation conditions described in Table 2, except the bubble and algal sizes. For the simulation of the bubble size effect, the bubble size was set up from 10 to 70 μm in radius for five different algal particle sizes: 9, 35, 50, 75, and 100 μm in radius. The simulation of the algal particle size effect was conducted in the range of algal size of 10–70 μm in radius, for five different bubble sizes: 9, 35, 50, 75, and 100 μm in radius. The simulation results are shown in Figure 2. Figure 2 presents the effect on the efficiency of the collision, the attachment, and the collision-attachment due to the bubble size and the algal particle size. The collision efficiency peaked when R was close to 1 and decreased as R was reduced. The attachment efficiency for the all algae became higher for larger bubble size. The conditions were not Stokes flow any more as the Reynolds number was over 1. According to the model assumptions, Case A was inapplicable under these conditions and there was a lack of smoothness when Case A was converted into Case B. Therefore, further detailed study requires a model description for micro-hydrodynamics considering potential flow and intermediate flow as well as Stokes flow. Smaller bubbles were effective on smaller algae, and bubbles much larger than the algae reached the maximum efficiency as R was closer to 1.

Also, simulations were conducted to examine sensitivity of collision-attachment efficiency to algal density and ionic strength, and the simulation conditions used were the same as the standard simulation conditions except for the following parameters: the bubble size was considered as 60 μm in radius instead of 42 μm, the algal radius was distributed from 20 to 120 μm, several different algal densities were adopted from 473.4 kg m^{-3} (PD0) to the final 7473.4 kg m^{-3}

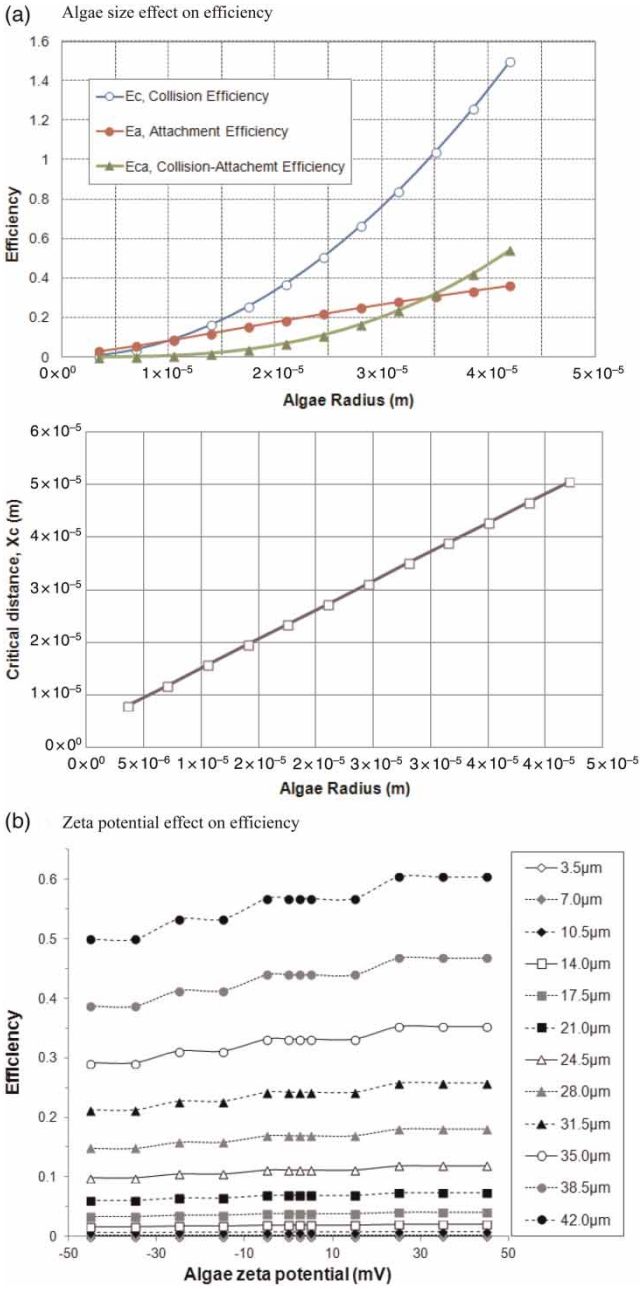

Figure 1 | Sensitivity of efficiency to parameters for Case A.

(PD7) with a 1,000 kg m^{-3} increment, and two ionic strength values, 0.003 and 0.1, were used. The collision-attachment efficiency was changed by increasing the algal density in Figure 3 and the ionic strength in Figure 4 for Case A and Case B.

In Figure 3, Case A was run for $R \leq 1$ ($r_p \leq r_b$), while Case B was conducted when $R > 1$ ($r_b < r_p$). PD0 and Is0 as the standard cases were compared with other cases. In Case A, the efficiency was inclined to rise and it grew slowly as R was increased or the algal size grew, while the efficiency increased suddenly as the algal density increased. However, the tendency of the efficiency to increase was indicated from smaller algal size as the algal density was increased. There was no influence on the efficiency due to the different algal densities from PD0 to PD2, the efficiency began to increase at the algal radius 50 μm for PD3, 40 μm for PD4 and PD5, and 30 μm for PD6 and PD7, and the growing trend of the efficiency was indicated by a somewhat gentle slope as the algal density increased. Unlike Case A, the efficiency for Case B tended to decrease as the algal size grew. For PD0 and PD1, the efficiency reached the maximum value when $R = 1$, decreased to its lowest at $R = 1.7$, and increased to the maximum again at $R = 2$. The efficiency for PD2 started to rise to a maximum at $R = 1.17$ and decreased again to the same level of PD3 to PD7. In the case of PD3 to PD7, the efficiency reached its peak at $R = 1$, declined as the algal size grew larger, and changed slightly only at $R = 1$. A similar situation appeared in the case of the ionic strength as shown in Figure 4, but the degree of alteration of the ionic strength was very slight. The collision-attachment efficiency calculated in this study would be applied as the initial collision-attachment coefficient in a model for PBT to estimate the flotation efficiency of the particle.

In summary, recent interest in flotation is in harvesting microalgae as a biofuel resource. Among practical techniques of algae harvesting used in industry, flotation techniques are very useful, including DAF and dissolved CO_2 flotation (DCF). Based on the separation characteristics, conditions to form auto-flocculation are predicted to obtain the optimal flotation efficiency. In particular, the algal mass collected by CO_2 micro-bubbles without dosing coagulants is pure and has a decided advantage for the material of various manufacturing processes. This study aimed at determining the feasibility of CO_2 bubbles as an algae particle separation collector in a flotation process and providing useful information for effective algae harvesting by describing optimal operation conditions of DCF and DAF, and understanding auto-flotation conditions due to a life cycle of *Spirulina* without dosing coagulants. For this purpose, a computational model (SCM) to determine collision-attachment efficiency between a particle and single bubble was simulated to evaluate the sensitivity of parameters in providing the optimal conditions in operating ranges of the DCF process, such as zeta potential, particle size, bubble size, ionic strength, and so on. Simulations estimated that limited critical distance was linearly influenced by algal size growth. Also, collision, attachment, and

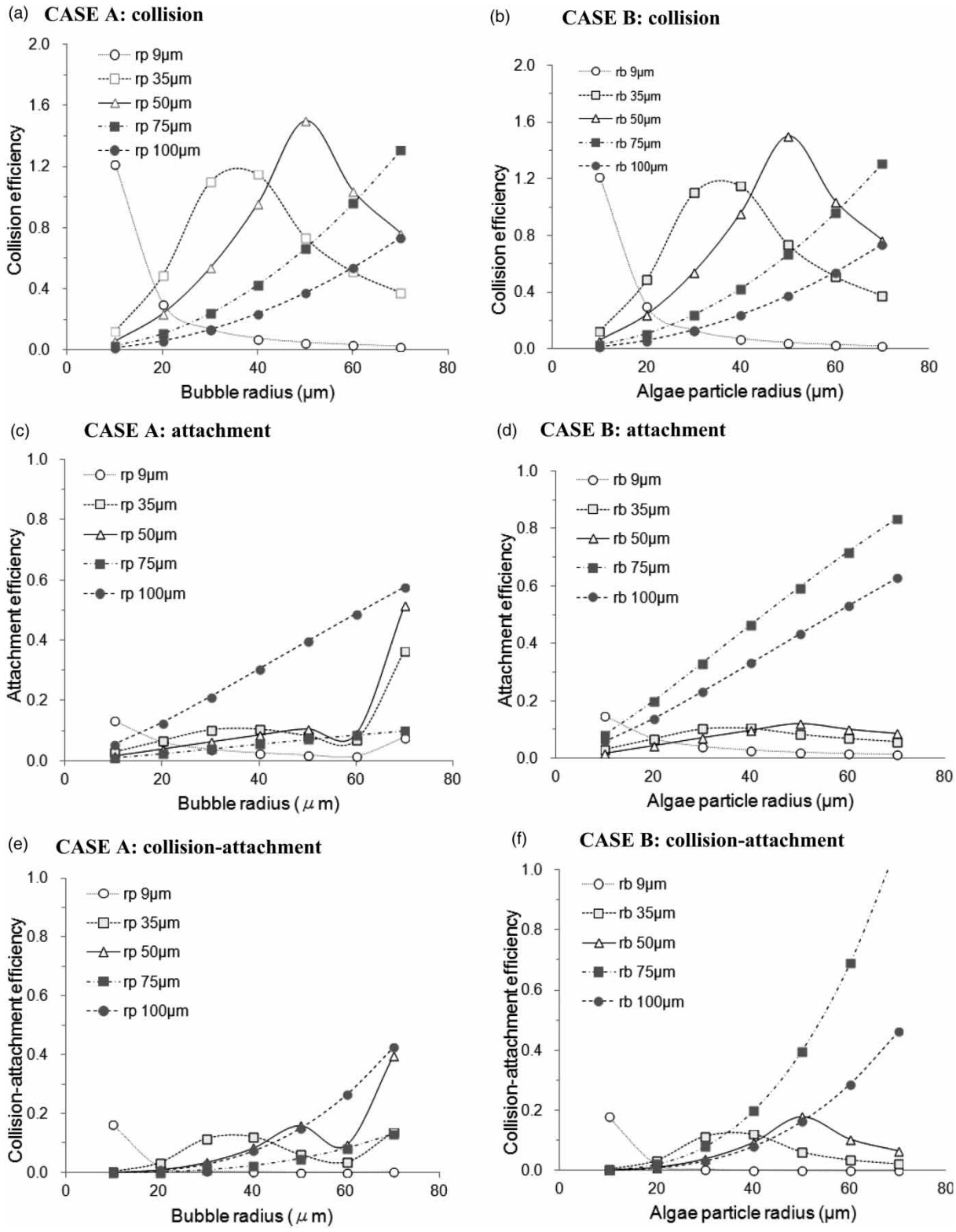

Figure 2 | Size effect on efficiency for Case A and Case B.

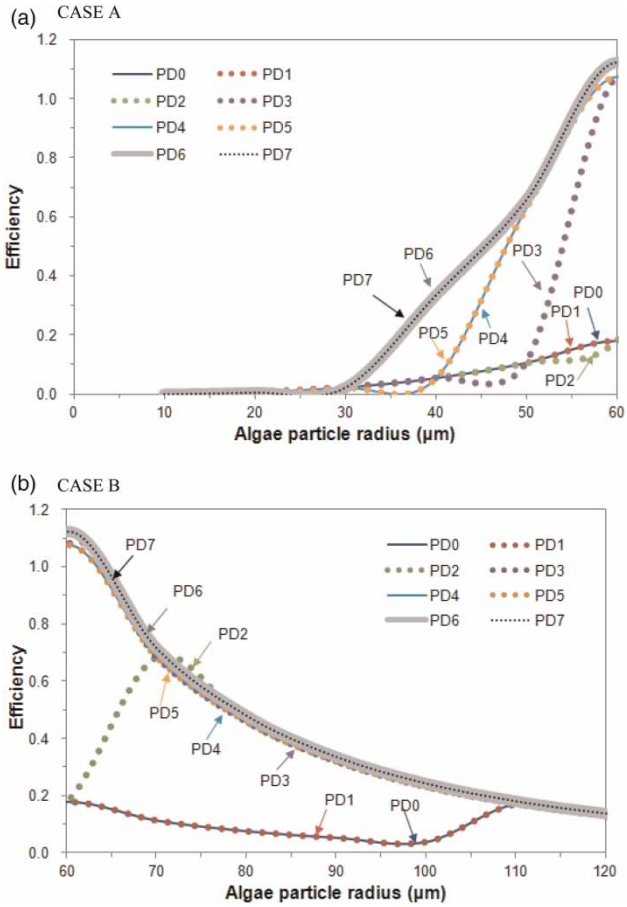

Figure 3 | Sensitivity of efficiency to particle density.

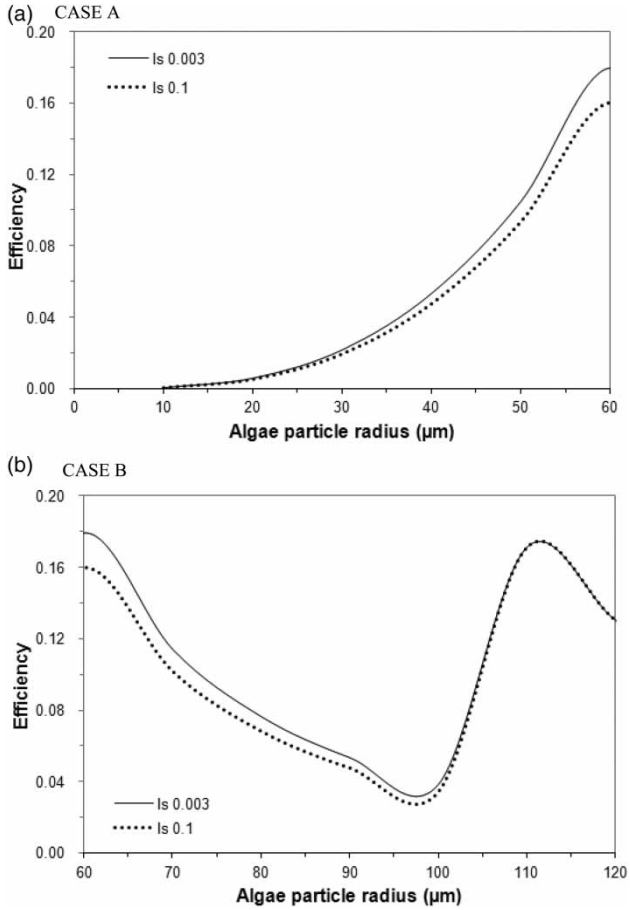

Figure 4 | Effect of ionic strength on efficiency.

collision-attachment efficiencies were determined according to algal size and algal zeta potential.

CONCLUSIONS

This study provided useful information for effective algae harvesting by describing optimal operating conditions of DCF and DAF as a function of zeta potential, particle size, bubble size, ionic strength, etc., and for understanding auto-flotation conditions due to a life cycle of *Spirulina* without dosing coagulants. It also verified the feasibility of using CO_2 bubbles in a flotation process to collect algae particles. Simulations estimated that limited critical distance was linearly influenced by algal size growth. Also, collision, attachment, and collision-attachment efficiencies were determined according to algal size and algal zeta potential. Larger algal size led to wider amplification of the efficiency as the algal zeta potential moved to positive values. Case A and Case B were tested for the sensitivity of efficiency to algal density and ionic strength with the growth of the algal size. Case A was inclined to rise, while Case B tended to decrease. The collision-attachment efficiency calculated in this study might be used for the initial collision-attachment coefficient in a model for PBT to estimate the flotation efficiency of the particle. The best collision-attachment efficiency was obtained when the micro-bubble size was similar to the microalgae size, and this result coincided with the previous study (Han *et al.* 2001). Also, the efficiency was better for higher positive algae zeta potential, much higher algae density, and lower ionic strength. However, the computational flotation model is limited to an infinitesimally small particle and a solid surface. Recent interest in DAF and DCF extends to harvesting the microalgae with a relatively soft film surface. Taki *et al.* (2004) suggest electrophoresis of the particle with soft surface characteristics, potential distribution within a layer of surface charge, and a theoretical form of electropherogram. Through experimental examination, they propose relations with the zeta potential of the phytoplankton cell surface, particle size,

and pH. Also, they emphasize that a more realistic interpretation will be possible if a theoretical model is established with consideration of the smooth surface factor as more important than the zeta potential of the cell surface and the surface charge state as very different according to the algae species, cell size, and so on. Therefore, further study in modelling flotation to harvest microalgae needs to consider not only the hard surface but also the soft film surface in the detailed micro-hydrodynamics of fluid for potential flow and intermediate flow, as well as Stokes flow reviewed by Firouzi *et al.* (2011).

ACKNOWLEDGEMENTS

This research (NRF-2012R1A1A4A01010342) was supported by the National Research Foundation of Korea (NRF) with grants from the Ministry of Education in Korea, 2013.

REFERENCES

Chisti, Y. 2008 Biodiesel from microalgae beats bioethanol. *Trends in Biotechnology* **26**, 126–131.

Demazel, D. 2008 *Use of Algae as an Energy Source*. Nordic Folkecenter, Denmark. http://www.folkecenter.net/mediafiles/folkecenter/pdf/Report_algae.pdf.

Edzwald, J. K. 2010 Dissolved air flotation and me. *Water Research* **44**, 2077–2106.

Ferrell, J. S. R. & Valerie, R. 2010 *National Algal Biofuels Technology Roadmap*. Biomass Program, Office of Energy Efficiency and Renewable Energy, US Department of Energy, Washington, DC.

Firouzi, M., Nguyen, A. V. & Hashemabadi, S. H. 2011 The effect of microhydrodynamics on bubble–particle collision interaction. *Minerals Engineering* **24**, 973–986.

Gaudin, A. M. 1957 *Flotation*. McGraw-Hill, New York.

Han, M. Y., Kim, W. T. & Dockko, S. 2001 Collision efficiency factor of bubble and particle (α_{bp}) in DAF: theory and experimental verification. *Water Science and Technology* **43** (8), 139–144.

Ho, N. F. H. & Higuchi, W. I. 1968 Preferential aggregation and coalescence in heterodispersed systems. *Journal of Pharmaceutical Science* **57** (3), 436–442.

Hogg, R., Healy, T. W. & Fuerstenau, D. W. 1966 Mutual coagulation of colloidal dispersions. *Transactions of the Faraday Society* **62**, 1638–1651.

Kwak, D.-H., Yoo, Y.-H., Yoo, D.-H. & Kim, M.-S. 2011 Application of carbon dioxide bubbles as a particle collector for flotation process in water treatment. In: *Proceedings of ISWA International World Congress*, 17–20 October, EXCO Daegu, Korea.

Kwak, D.-H. & Kim, M.-S. 2013a Feasibility of carbon dioxide bubbles as a collector in flotation process for water treatment. *Journal of Water Supply: Research and Technology-AQUA* **62** (1), 52–65.

Kwak, D.-H. & Kim, M.-S. 2013b Evaluation of model simulation and field test on collision efficiency for operational factors in dissolved air flotation process. *Separation Science and Technology* **48** (15), 2243–2251.

Levich, V. G. 1962 *Physicochemical Hydrodynamics*. Prentice-Hall, Englewood Cliffs, NJ, pp. 213–434.

Nguyen, A. V. 2011 Particle–bubble interaction in flotation. In: *Bubble and Drop Interfaces: Progress in Colloid and Interface Science*, R. Miller & L. Liggieri (eds). Brill, Leiden, The Netherlands, pp. 351–384.

Packham, R. F. & Richards, W. N. 1972 *Water Clarification by Flotation-1*. Technical Paper 87, Water Research Association, Medmenham, UK.

Taki, K., Ishiyama, Y., Dockko, S. & Kim, H. 2004 DAF technology for various kind of plankton removal from eutrophic lakes. *Journal of the Korean Society of Water and Wastewater* **18** (2), 247–253.

Wiley, P. E., Brenneman, K. J. & Jacobson, A. E. 2009 Improved algal harvesting using suspended air flotation. *Water Environment Research* **81** (7), 702–708.

Xu, L., Wang, F., Li, H.-Z., Hu, Z.-M., Guo, C. & Liu, C.-Z. 2010 Development of an efficient electroflocculation technology integrated with dispersed-air flotation for harvesting microalgae. *Journal of Chemical Technology Biotechnology* **85** (11), 1504–1507.

First received 14 January 2014; accepted in revised form 19 March 2014. Available online 3 April 2014